Brazilian Journal of Microbiology
https://doi.org/10.1007/s42770-025-01612-1

FOOD SAFETY AND QUALITY - RESEARCH PAPER

Carbon-dot pequi-nut in the development of immunosensor to detect pathogenic bacteria

Rachel Menezes Castelo[1] · Marília de Albuquerque Oliveira[2] · Roselayne Ferro Furtado[3] · Bruno Peixoto de Oliveira[4] · Lucas Vinicius Leite Martoni[5] · Terezinha Feitosa Machado[6] · Celli Rodrigues Muniz[7] · Flávia Oliveira Monteiro da Silva Abreu[8] · Sérgio Antônio Spinola Machado[5] · Airis Maria Araújo Melo[9] · Huai N. Cheng[10] · Atanu Biswas[11] · Carlucio Roberto Alves[1]

Received: 22 August 2024 / Accepted: 2 January 2025
© The Author(s) under exclusive licence to Sociedade Brasileira de Microbiologia 2025

Abstract
Carbon dots in biosensing have advanced significantly, adding improvements to different detection techniques. In this study, an amperometric immunosensor for *Salmonella* Thyphimurium was designed using antibodies labeled with carbon dots (Cdots) from pequi almond (*Caryocar brasiliensis*). Cdots were synthesized by pyrolysis and characterized by FTIR, UV/fluorescence, electrochemistry, zeta potential, and transmission electron microscopy (TEM). A particle size of 6.80 ± 2.13 nm was estimated, and the zeta potential was −47.4 mV, indicating the preponderant presence of acidic groups, as confirmed by FTIR. The impedance evaluation of the response of biosensors assembled for live (Rct = 13.4 kΩ) and dead (Rct = 499.7 Ω) *Salmonella* showed a significant difference in their values, in agreement with chronoamperometric analyses, which had their current values drastically reduced from −2.2 mA (live) to 0 mA (dead). An analytical curve for *Salmonella* was established with the limit of detection lower than 1 CFU/mL. This electrochemical biosensor using pequi carbon dots for antibody labeling showed promising results for detecting the pathogen. Thus, carbon dots can be used as substitutes for enzymes in labeling antibodies used in the design and production of sensors.

Keywords Carbon dots · *Caryocar brasiliensis* Cambess · Immunosensor · Pequi-nut · *Salmonella*

Introduction

Ensuring access to safe and healthy food for all is a global challenge [1]. A major factor in food safety is the detection and prevention of pathogenic contamination, in food products [2]. It is known that salmonellosis can cause health risks with symptoms that can last for up to a week [3]. Salmonellosis is often associated with symptoms similar to the stomach flu, including nausea, vomiting, abdominal cramps and bloody diarrhoea. It can also cause headache, fever and muscle aches. Prolonged fluid loss can lead to dehydration, especially in young children and the elderly. In severe cases, deaths have been reported, especially in vulnerable groups such as young children, the elderly and people with weakened immune systems [4]. Thus, *Salmonella* detection in food samples is an important analysis. The bacteriological assay is considered the gold standard for *Salmonella* detection, but this assay involves several steps and can take several days to complete [5]. Alternative detection methods for *Salmonella* Typhimurium have appeared in the literature, including ELISA [6], polymerase chain reaction (PCR) [7], surface-enhanced Raman scattering (SERS) [8], and graphene electrochemical immunosensor [9]. However, these methods often have drawbacks, such as time-consuming procedures, expensive equipment, and adequate training of technicians. The need to explore simple, rapid, cost-competitive, high-sensitivity, and specificity detection methods for pathogenic bacteria has motivated the development of electrochemical biosensors for *Salmonella*.

Electrochemical sensors appear as an effective route for replacing the previously mentioned methods, as they can detect a single chemical [10, 11] or biological molecule [12,

Communicated by Uelinton Manoel Pinto.

Extended author information available on the last page of the article

Published online: 15 January 2025

13]. Amperometric immunosensors have been preferred for their easy handling and ability to work with specific potential, thereby greatly reducing the interference of other chemical species [14–16]. From a microbiological safety perspective, the use of these biosensors minimizes the need for sample handling and reduces the risk of human contamination, making them promising technologies for the food industry. However, most of these biosensors are still at the prototype stage [17, 18], and have not yet been approved by international certification bodies or been implemented on a large scale. The detection of microorganisms by biosensors can be either direct or indirect. In direct detection, the bioactive molecule interacts directly with the microorganism, while indirect detection focuses on monitoring microbial metabolites via biochemical reactions that occur on the transducer surface[19]. Electrochemical biosensors designed for indirect detection evaluate parameters such as changes in pH, oxygen consumption, ion concentration, potential difference, current or resistance. The transducer can detect oxygen consumption and the formation or degradation of electrochemically active metabolites [19].

Previous works on immunosensors for *Salmonella* detection have shown high sensitivity without the need for a sample pre-enrichment step using an enzyme-labeled antibody [20, 21]. The literature has also shown a variety of functionalization in the construction of immunosensors involving nanoparticles [22–24], some incorporating carbon dots as biomarkers, which can be switched "on-off" and highly sensitive [25], reaching limits of detection in the range of fg/mL [26].

Carbon dots are nano-sized carbon-based materials that have gained significant attention in nanotechnology and materials science. These tiny dots, typically ranging from a few to a few dozen nanometers in size, exhibit unique optical, electronic, and chemical properties, including their easy surface functionalization, low-cost synthesis, and visible light absorption [27, 28]. Recently, pequi carbon dot was developed and tested for identification of bacteria by flow cytometry [29]. This kind of carbon dot in electrochemical biosensors is being reported for the first time in this work.

In particular, an electrochemical immunosensor functionalized with nanoparticles synthesized from pequi nut can be advantageous due to possibility of adding value to this agricultural product and because it provides facile electron transfer paths and has adequate conductivity characteristics [30]. These features open the possibility of developing sensitive devices with detection limits equivalent to or lower than those needed for identifying *Salmonella* or similar pathogens [9, 14, 31]. In this work, carbon dot was used as a marker of secondary antibody in the analytical response of an immunosensor for *Salmonella* detection. This procedure is necessary for amperometric analysis given that the antigen-antibody interaction does not involve redox reactions to have measurable current variations correlating to the presence of the analyte.

Materials and methods

Preparation and characterization of Carbon dots

Pequi fruits were purchased from a local market in Fortaleza. The pequi almonds were first separated manually from the fruit. Carbon dots synthesis from pequi almonds followed the bottom-up approach through the microwave pyrolysis. 2 g pequi almond was macerated with H_2PO_4 (40%) and heated in the microwave for 1.5 min at 600 W. Then, 20 mL of ethanol and 1 mL of 2 M NaOH were added, filtered on a filter paper, and centrifuged at 11,000 rpm for 20 min. The supernatant was discarded, and the precipitate dialyzed in distilled water for 48 h. The dialyzed sample was filtered using a 22-µm pore filter and then lyophilized. For the quantitative determination of the chemical elements C, H, N, and S present in a sample, a ThermoScientific Elemental Analyzer (model FlashSmart) was used, with external calibration involving methionine, BBOT, sulfanilamide and cystine as calibration standards.

The synthesized material was characterized by Fourier transform infrared spectroscopy (FTIR) using an attenuated total reflectance detector in the wavelength range of 400–4000 cm^{-1} and resolution of 4 cm^{-1} on an FTLA 2000-102-ABB- BOMEN spectrometer (ABB Group, Quebec, Canada).

The particle size analysis was performed using a transmission electron microscope (TEM), model Vega 3, made by Tescan (Brno, Czech Republic). The sample was diluted 1:50 v/v, gridded for 3 min, and stained with phosphotungstic acid for 3 min. The particle size calculation was achieved by imageJ software.

UV-Vis analyses were performed using a Shimadzu UV-2600i UV-visible spectrophotometer, and the measured wavelength range was 190–800 nm.

Fluorescence analysis was carried out on a Shimadzu RF-6000 spectrofluorimeter with excitation frequency at 200–400 nm, and emission in the range of 400 to 800 nm, with a scanning speed of 6000 nm/s and excitation and emission slits of 5.0 nm.

The quantum yield (QY), a parameter for comparing the photoluminescence of Cdots, was calculated by the ratio between the number of photons absorbed and the number of photons emitted by a material through Eq. 1.

$$QY = QYs\left(\frac{I}{I_s}\right)\left(\frac{A_s}{A}\right)\left(\frac{n}{n_s}\right)^2 \quad (1)$$

where I is the integrated emission intensity, A is the absorption intensity at the excitation wavelength, n is the refractive index of the solvent, and the subscript s is related to the value of the standard fluorescent molecule.

Antibody purification and carbon dot-labeled antibodies

Polyvalent anti-*Salmonella* serum Poli A-I and Vi purchased from Difco® were purified by precipitation with $(NH_4)_2SO_4$ with 45% saturation. The serum was reconstituted in 3 mL of NaCl (0.85%) followed by the addition of 1.662 g of $(NH_4)_2SO_4$. The obtained solution was kept under stirring for 30 min, refrigerated for 24 h, and subsequently centrifuged at 10,000 rpm (15,303 x g) for 30 min at 4 °C. The precipitate was dialyzed against PBS (10 mM pH 7.4) for 24 h. After dialysis, its concentration was determined in a NanoDrop 2000 spectrophotometer (Thermo Scientific).

Cdot-labeled antibodies were preparated from Cdot dispersed in buffer solution (pH 7.4) with the antibody using the proportion 1:6 (antibody: Cdot, w/w).

Bacterial culture

Bacterial culture was prepared according to the method described by Melo et al. (2021) [32] with modifications. The strain *Salmonella* enterica serovar Typhimurium (ATCC® 51812) was cultivated in BHI at 37 °C for 24 h. The resulting bacterial suspension of unknown concentration was centrifuged for 30 min at 5000 rpm, and the supernatant was discarded. The pellet was washed with sterile PBS pH 7.4 and then used to prepare a suspension with sterile PBS, in which bacterial concentration was adjusted using the McFarland turbidimetric method. The standard bacteria suspensions for the calibration curve were prepared by successive dilution. The concentrations of standard dispersions were confirmed using the conventional plate counting method with 10^5 to 10^8 CFU mL^{-1} suspension. The standard dispersions were stored at 4 °C until use, and all the experiments were done in triplicate.

Biosensor preparation

The assembly of the immunosensor was performed on the surface of a disposable gold electrode, using the self-assembled monolayers (SAMs) technique, according to the method given by Melo et al. [21] with adaptations.

Screen-printed electrodes Dropsense (C220AT®) were immersed in 10 mM cysteamine ethanolic solution (cys) for 3 h. Then, the electrode was immersed in a solution of protein A (protA) 7.5 mg mL^{-1} of *Staphylococcus aureus* containing N-hydroxysuccinimide/N- (3-dimethylamino propyl) -N'-ethylcarbodiimide (EDC/NHS) (2 mM/ 5 mM) for 1 h. Before immersion, the NHS/EDC solution was kept for 30 min at room temperature and for 30 min; then, the prot A was added to react for one hour. The solution was left for one hour, and the electrode was immersed in the solution for 1 h, called modified cys-protA electrode. After that, the electrode was washed with 10 mM phosphate buffer (PBS) (pH 7.4). The modified electrode was then immersed overnight in a solution of anti-*Salmonella* (AS) (2 mg mL^{-1}) under refrigeration. The non-specific binding was blocked with 1% bovine serum albumin solution (w/v) for 1 h. Finally, the modified electrode was immersed in an anti-*Salmonella*-Cdot solution in a ratio of 1:6 w/w for 1 h (Fig. 1).

Electrochemical measurements were made using Autolab/PGSTAT12 potentiostat/galvanostat (Ecochemie, Netherlands) coupled to a computer and controlled by NOVA 2.1.3 software (Ecochemie, Netherlands (Metrohm, Switzerland)). Chronoamperometry studies were performed at a constant potential of 0.4 mV for 120s. The analysis of variance (ANOVA) [24] was used to analyze the standard curve for *Salmonella* concentrations. The limit of detection (LOD) was calculated using Eq. 2.

$$LOD = YB + 3.3SB \quad (2)$$

Where Y_B is the linear coefficient, and S_B is the standard deviation of the blank [33].

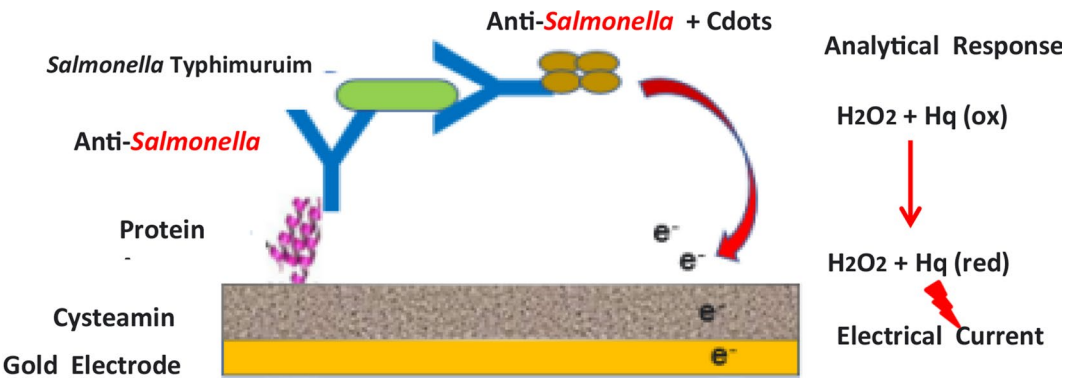

Fig. 1 Immunosensor assembly based on anti-*Salmonella*-Cdot and the analytical response (ox) oxidation and (red) reduction

Electrochemical impedance spectroscopy (EIS) data were acquired with a PGSTAT 302 potentiostat/galvanostat (Ecochemie, Netherlands) system, controlled by FRA2 software (Metrohm, Switzerland). EIS experiments were performed, in 0.1 mol L^{-1} KCl solution containing 5.0 mmol L^{-1} $K_3[Fe(CN)_6]/K_4[Fe(CN)_6$, under the open circuit potential (OCP), in the frequency range between 0.1 Hz and 100 kHz with an amplitude of 10 mV and under the open circuit potential (OCP) conditions in 0.1 mol L^{-1} KCl solution containing 5.0 mmol L^{-1} $K_3[Fe(CN)_6]/K_4[Fe(CN)_6]$. The light source was an UV LED (9 W) operated by a lab-made controller board (UNO) integrated into a relay and programmed by Arduino software.

Statistical analysis

Three replications were performed in the assays and used to obtain mean and standard deviation results. The linearity was confirmed by ANOVA using Origin 8.0.

Results and discussion

Carbon dots characterization

The synthesis of Cdots from the pequi almond showed a reaction yield of 5%. Its quantum yield, calculated from fluorescence and UV-Vis spectra, was 9% (Fig. 2b). Since the elemental analysis indicated a nitrogen content of 11% and a carbon/nitrogen ratio of 1/3, nitrogen in Cdot significantly affected the quantum yield value. From a comparison of the Cdots obtained from the pequi almond with other Cdots obtained from natural sources, this QY value was higher than or compatible with the quantum yield of Cdots synthesized from the *Cissus quadrangularis* leaf, which was above 5% [34], cellulose fibers where QY reached the value of 1% [35], and quantum dots extracted from fig leaves with 3% QY [36]. According to fluorescence spectroscopy, the increase in the excitation wavelength (Fig. 2a) increased the luminescent intensity of the Cdots. It shifted the maximum emission to a region closer to red, known as

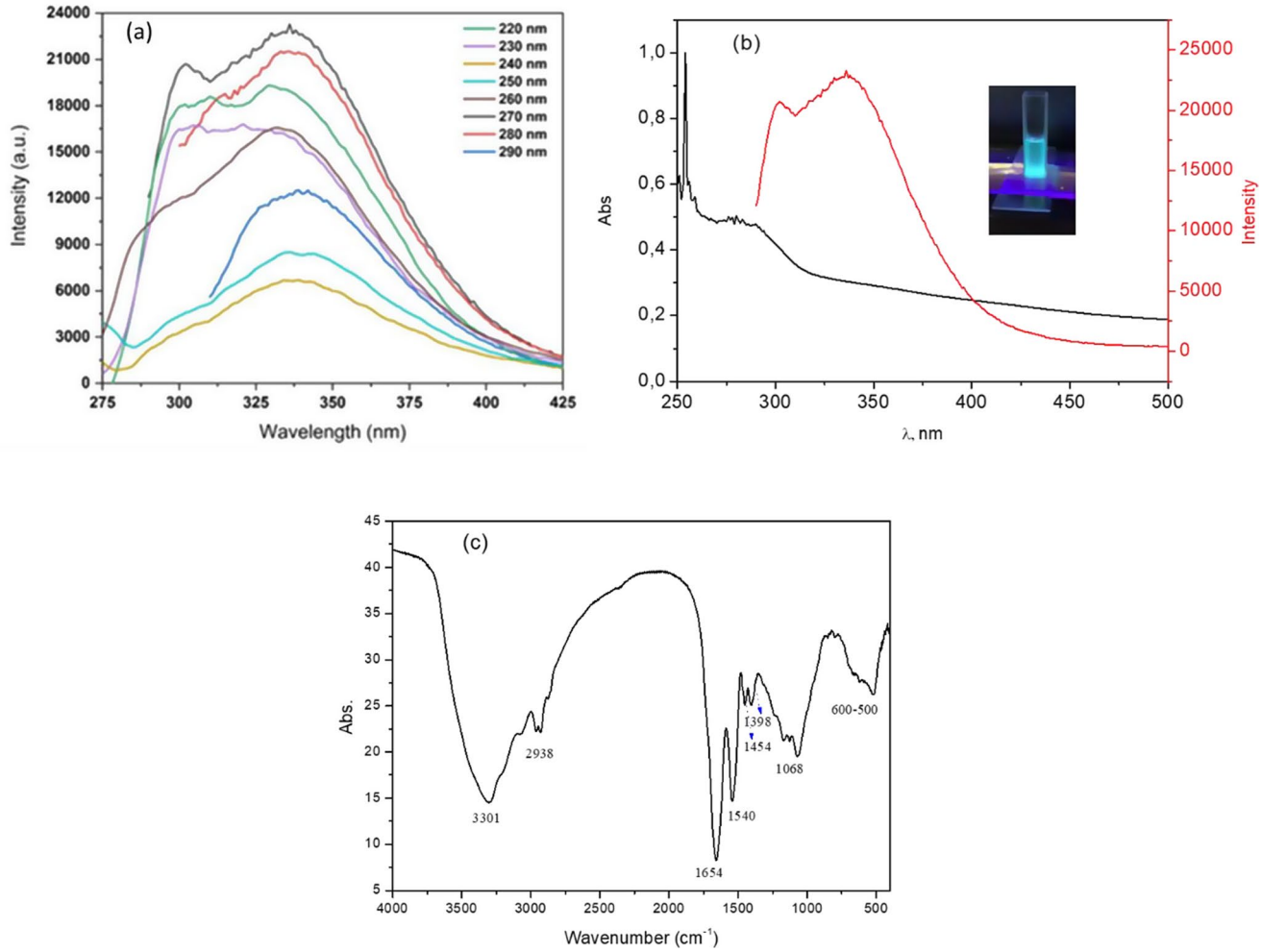

Fig. 2 (**a**) Fluorescence emission spectra of Cdots; (**b**) UV-Vis and fluorescence spectra at λ = 270 nm; (**c**) FT-IR spectrum of Cdots

the bathochromic effect [37]. This excitation wavelength-dependent photoluminescence behavior is characteristic of Cdots based on natural sources [38, 39] and may be linked to the nitrogen content of the Cdots sample [40, 41].

The Fig. 2a shows that in 290 nm region approximately, excitation occur and its observed a decrease in luminescent intensity, fact that may be related to quantum confinement, size distribution, or the presence of emitting traps on the Cdot's surface [42]. At wavelength of 340 nm the maximum emission peak occurred, representing an average fluorescence intensity of 23,314 a.u. Groups on the Cdots surface, especially those containing oxygen, nitrogen, and hydrogen atoms, can have different energy levels that make the emission dependent on the excitation energy. In addition, the fluorescence emission can change due to particles of different sizes and emissive sites' distribution on its surface [43].

The UV-vis absorption spectrum (Fig. 2b) showed maximum absorption in the UV region, which decreased in the visible region. Cdots have characteristic peaks (UV) at 300 nm in the π - π* electronic transition region corresponding to sp^2 and n - π* carbon bonds of surface carbons with structures containing nitrogen and/or oxygen [44], agreeing with the emission spectrum at region between 325 and 340 nm, indicating that the blue band in the photoluminescence results from transitions in the Cdots core and defect surface with sp^3 hybridization, respectively [45].

The infrared spectrum (Fig. 2c) showed intense -OH bands at 3400 cm^{-1}. The presence of C=O bonds of the carboxylate ion and C=C of the carbon structure was confirmed by absorptions at 1654 and 1391 cm^{-1}, respectively. Another high-intensity band was observed at 2930 cm^{-1}, which can be attributed to the asymmetric stretching of C-H bonds in the aliphatic portion of the Cdot's surface. The collapsed band can characterize the amino groups at 3200 cm^{-1} and the region with several peaks at 600–500 cm^{-1}, corresponding to the N-H bonds of primary amine [29].

Through transmission electron microscopy (TEM) analysis (Fig. 3), the Cdots were found to have a spherical shape in the regions where they appeared dispersed. The measured particle size was 6.80±2.13 nm. The size and form of the Cdots are in agreement with other studies [46, 47]. The zeta potential of Cdots in aqueous media was −47.4±0.3 mV, suggesting the preponderant presence of carboxylic acid groups on the surface, and other oxygenated functional groups [48]. The highly negative value of the zeta potential means that the electrostatic forces are predominantly repulsive, indicating that the system has a high stability against aggregation. These results agree with the TEM image,

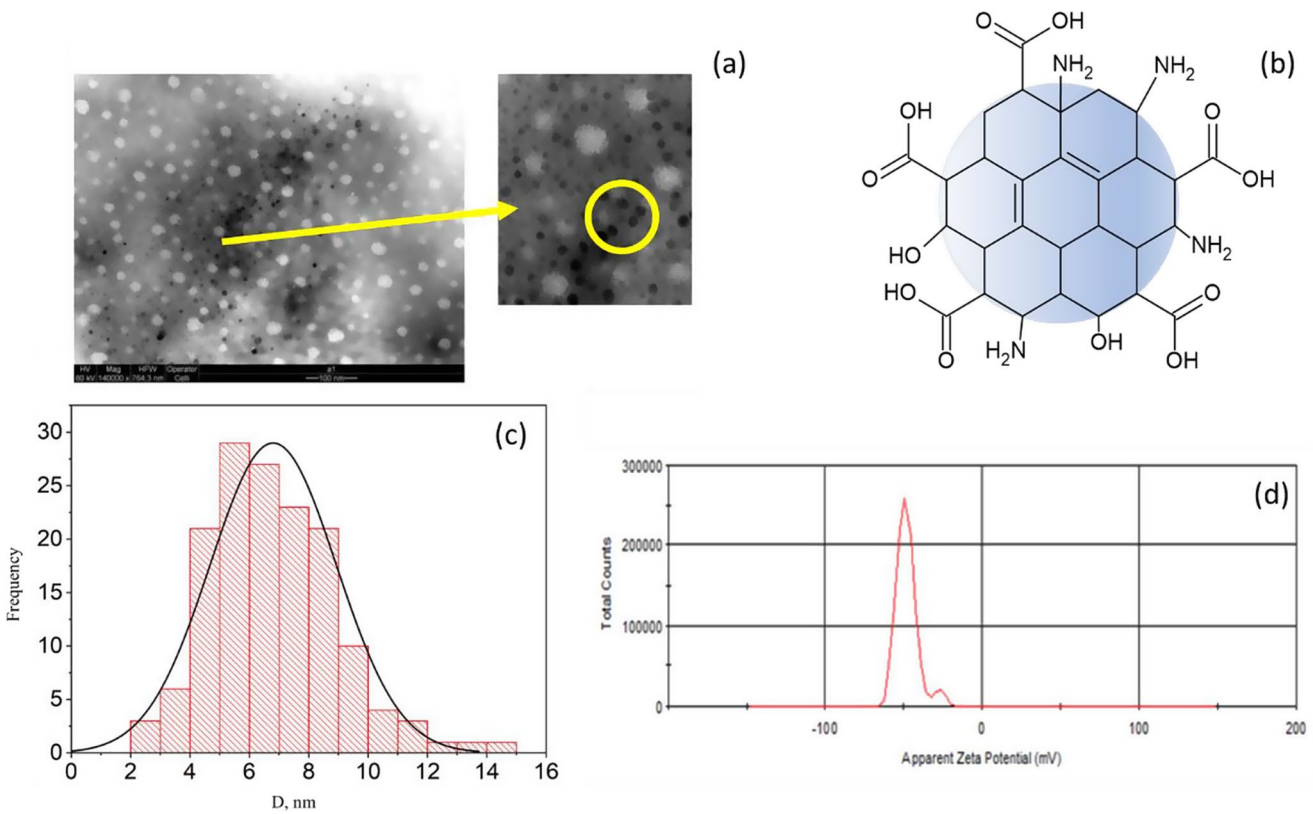

Fig. 3 (**a**) Transmission electron micrograph of carbon dots diluted in water at a ratio of 1:50 v/v, deposited on a grid for 3 min and stained with phosphotungstic acid for 3 min; (**b**) probable structure of the carbon dot with carboxylic acid groups around it; (**c**) statistical particle size distribution; (**d**) distribution graph of the zeta potential of the carbon dots solution in water

where Cdots were observed to be well dispersed, in agreement with the earlier findings of [49].

Performance and characterization of the biosensor

Chronoamperometry analysis

The chronoamperometric behavior (Fig. 4a) for the biosensor assembled and tested with live and dead *Salmonella* showed a drop in the electrical signal from −2.2 mA to zero. This observation is reasonable, as *Salmonella* is a filamentous bacterium that, when alive, has its flagella always in movement, capable of interacting with the antibody. After slow pasteurization, the bacteria cannot interact with the antibody and may precipitate out of the medium; thus, the device cannot present any electrical signal. Biosensor performance evaluation tests were carried out on samples with different concentrations of *Salmonella*, simulating a contaminated sample at concentrations of 1–107 CFU.mL^{-1} as represented in Fig. 4b. The mass ratio of Cdots and antibody for the assembly of the immunosensor in the proportion of 6:1 (m/m) made it possible to visualize the decrease in the electrical signal with the increase in the concentration of *Salmonella*. Thus, it was possible to construct an analytical curve with an amperometric response of the immunosensor at different concentrations of *S.* Typhimurium, thereby establishing a relationship between the current signal (A) and the analyte concentration (CFU.mL^{-1}) with a correlation index (R) equal to 0.98 [24].

The immunosensor was able to distinguish between different concentrations of *Salmonella* ($p<0.05$). ANOVA [50] confirmed its linearity, so the quantitative behavior of the biosensor for the pathogen could be confirmed. The LOD of the device was < 1 CFU/mL, indicating a good sensitivity of the device, compared to biosensors assembled with the peroxidase enzyme with LOD 10 CFU/mL [21] and compared to syringe actuation biosensors using nuclear membrane filtration and nanozyme signal amplification, which despite its simpler assembly obtained a LOD of 12 CFU/mL [51]. Similar behavior to this study was seen in a paper on a gold nanocluster colorimetric aptasensor that was developed for the detection of *S.* Thiphymurium in eggs and exhibited a broad linear response in the concentration range of 10^1–10^6 CFU/mL with a detection limit as low as 1 CFU/mL [52].

Electrochemical impedance spectroscopy (EIS) analysis

The manufacturing process of the electrochemical biosensor was elucidated by EIS in $[Fe(CN)_6]^{3-/4-}$ at 5.0 mM. After assembling the biosensor with live *Salmonella* at a concentration of 1 CFU/mL and with dead *Salmonella*, previously pasteurized at 65ºC for 30 min [53, 54]., the impedimetric data for the two situations were collected and are shown in Fig. 5. Figure 5a shows the Rct measurements for ant-*Salmonella* (Rct = 10.4 KΩ), *Salmonella* (Rct = 61.7 KΩ), and the last step with ant-*Salmonella*-Cdot (Rct = 20.5 KΩ). As the electrode surface was modified, the Rct did not increase in an orderly fashion due to the non-conducting properties of these protein structures as well as the small size of molecules in each assembly step, e.g., cysteamine [55, 56]. However, a trend is observed in which there is an increase in resistance in *Salmonella* at low frequency and at the end of the assembly in ant-*Salmonella*-Cdot, where the resistance drops to 20.5 KΩ, giving evidence that Cdot has semiconductor properties. Various types of carbon (and quantum)

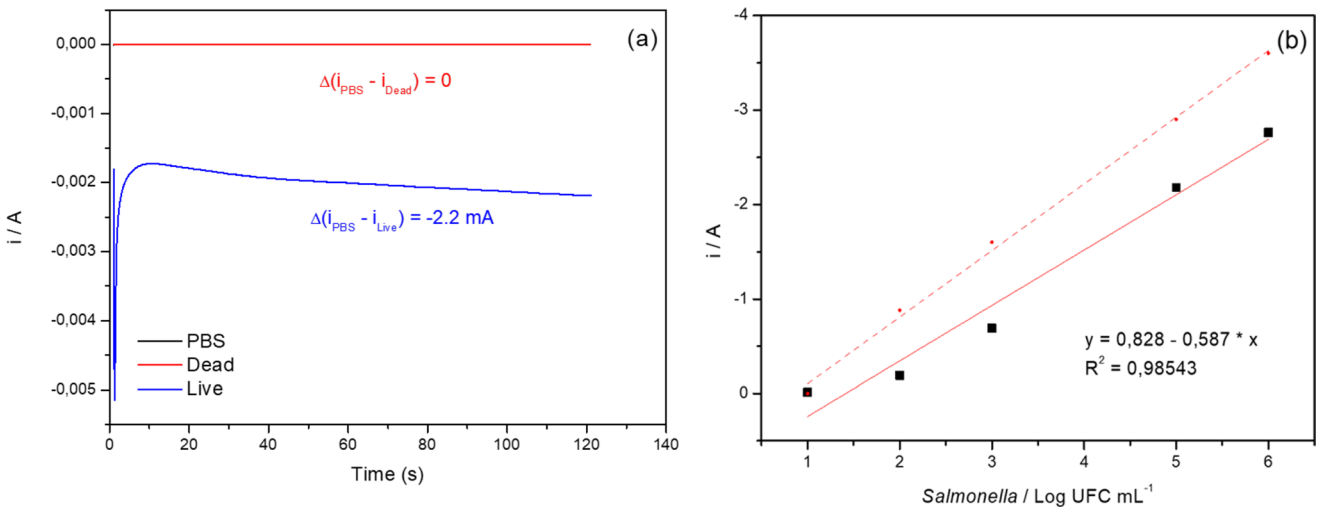

Fig. 4 (**a**) Amperometric response for biosensors in live and dead *Salmonella*. The chronoamperogram of the inactive *Salmonella* biosensor coincided with the PBS curve, providing zero difference; (**b**) Analytical curve for immunosensor assembled with Cdots-labeled antibody at m/m ratio of 1/6

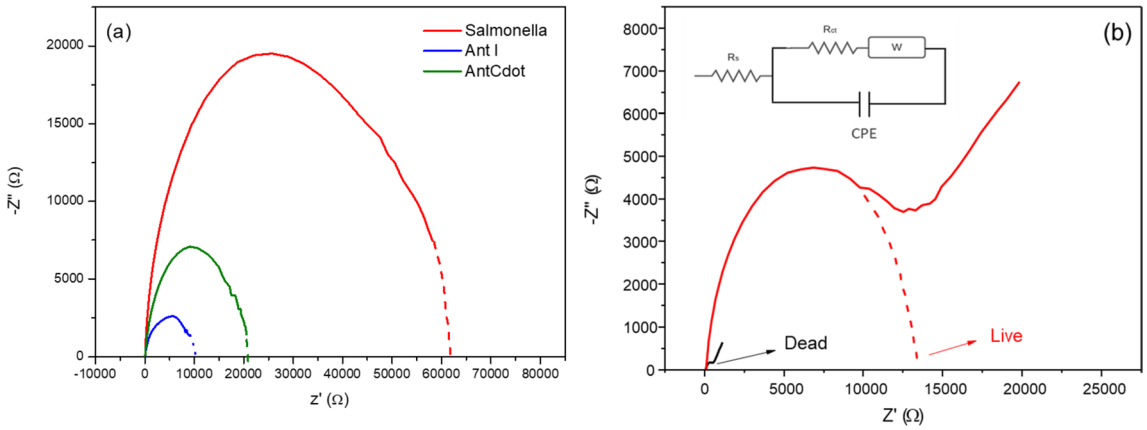

Fig. 5 (**a**) The typical Nyquist diagram for the biosensor formation steps; (**b**) Nyquist diagram for biosensors with live and dead *Salmonella* with a Randles circuit, for live only, comprising the uncompensated electrolyte resistance (Rs), in series with the dielectric layer capacitance (CPE), transfer resistance load (Rct) and Warburg impedance (W), in circuit form

dots with semiconductor characteristics have become potential new platforms for application as fluorescent probes [57]. For this system, the earlier literature reported that the value of quantum yield is directly related to charge transfer, as high quantum yield offers greater resistance to charge transfer because it has fewer electrons in the excited state to contribute to conductivity [58].

Additionally, unlike cysteamine, the BSA immobilization step (used as a blocking molecule for non-specific antibody sites during biosensor assembly) caused a significant increase in charge transfer resistance (curve not shown - Rct = 74.0 kΩ). This high resistance to electrical conductivity is due to the lack of electrons available in the excited state, and the protein forms a blocking barrier for the diffusion process on the modified electrode surface [59]. Thus, the protein layer is considered a porous insulating layer and can work like a capacitive element. Furthermore, the high protein adsorption density on the electrode surface leads to a small interface area (Rs), so the solution resistance within the protein layer interface is not negligible (Huang et al., 2019).

Figure 5b shows that the resistance of the biosensor for dead *Salmonella* (Rct = 499.7 Ω) gives a lower Rct value than the live bacteria (Rct = 13.4–20.5 KΩ in Fig. 5b, which gives the Nyquist diagram in the Randles circuit for the biosensor assembled with live *Salmonella*). The dead *Salmonella* shows that the bond between the pathogen and the antibody conjugated to Cdots is lost, thereby interrupting the passage of electrons. This behavior allows the device to avoid false-negative results that can be generated by the PCR technique, where its detection mechanism by DNA may cause a false-positive response even to dead bacteria [60]. Therefore, the biosensor described in this work becomes extremely important for applications in industrial processes for checking food quality, as it would not invalidate an entire batch of food materials because it differentiates between living and dead microorganisms [61].

Given the mandatory absence of *Salmonella* in food determined by health surveillance authorities, the biosensor developed in this research presents itself as an excellent alternative for rapid and accurate detection, allowing industries to quickly and safely make the food produced available to consumer markets. Thinking about the industrial sector, its use would bring benefits to food safety, quality control, speed up delivery logistics and ultimately make the industry more competitive in the food market.

Conclusions

Carbon dot technology represents an exciting new opportunity for innovation involving biobased materials. This article used antibodies labeled with Cdots from pequi almond to build a biosensor designed for *Salmonella* detection. The synthetic route to obtaining Cdots from pequi almonds was simple and quick, with a process yield of 5%. The size of the Cdots was 6.8 nm, compatible with the range determined for materials of this nature, with a spherical appearance and good dispersion. The quantum yield of 9% was satisfactory when compared to other similar materials in literature. The immunosensor developed with pequi Cdots could distinguish between different concentrations of live *Salmonella* ($p < 0.05$) if quantitative behavior for the pathogen was assumed. The LOD calculated for this device was ten times more sensitive relative to biosensors developed with the peroxidase enzyme, which places the biosensor in this work on the list of ultrasensitive devices. Another important aspect is that this device distinguishes live and dead *Salmonella*, and this is an advantage over other detection methods, like PCR analysis. The developed device has features such

as portability, ease of handling, fast response and accurate results, demonstrating great potential for application in the food production chain, from the field to the final product. Consequently, consumers would benefit from healthy and affordable products due to the shortening of production time, thanks to the agility of the production process with the use of biosensors as tools for monitoring food safety.

Supplementary Information The online version contains supplementary material available at https://doi.org/10.1007/s42770-025-01612-1.

Acknowledgements The authors are thankful to the Conselho Nacional de Desenvolvimento Científico e Tecnológico (CNPq) for the financial support granted through process nº 140459/2020-0. This study was financed in part by the Coordenação de Aperfeiçoamento de Pessoal de Nível Superior– Brasil (CAPES)– Finance Code 001.

Declarations

Competing interests The authors declare that they have no known competing financial interests or personal relationships that could have appeared to influence the work reported in this paper.

References

1. Stanaway JD, Parisi A, Sarkar K et al (2019) The global burden of non-typhoidal *Salmonella* invasive disease: a systematic analysis for the global burden of Disease Study 2017. Lancet Infect Dis 19:1312–1324. https://doi.org/10.1016/S1473-3099(19)30418-9
2. World Health Organization (WHO) (2024) Food safaty. In: https://www.who.int/news-room/fact-sheets/detail/food-safety
3. Giannella RA (1996) Medical Microbiology, 4th edn. Galveston, Texas
4. Ehuwa O, Jaiswal AK, Jaiswal S (2021) *Salmonella*, Food Safety and Food Hanpracticesctices. Foods 10:907. https://doi.org/10.3390/foods10050907
5. Corrêa IMO, Pereira LQ, Silva IGO et al (2018) Comparison of three diagnostic methods for *Salmonella enterica* serovars detection in chicken rinse. Pesquisa Veterinária Brasileira 38:1300–1306. https://doi.org/10.1590/1678-5150-pvb-5211
6. Hu J, Huang R, Wang Y et al (2018) Development of duplex PCR-ELISA for simultaneous detection of *Salmonella* spp. and *Escherichia coli* O157: H7 in food. J Microbiol Methods 154:127–133. https://doi.org/10.1016/j.mimet.2018.10.017
7. Ben Hassena A, Barkallah M, Fendri I et al (2015) Real time PCR gene profiling and detection of *Salmonella* using a novel target: the siiA gene. J Microbiol Methods 109:9–15. https://doi.org/10.1016/j.mimet.2014.11.018
8. Chuesiang P, Ryu V, Siripatrawan U et al (2021) Investigation of factors that impact the label-free surface-enhanced Raman scattering (SERS) for the detection and discrimination of *Salmonella* Enteritidis. https://doi.org/10.1016/j.lwt.2021.111962. LWT 150:
9. Feng K, Li T, Ye C et al (2022) A novel electrochemical immunosensor based on Fe3O4@graphene nanocomposite modified glassy carbon electrode for rapid detection of *Salmonella* in milk. J Dairy Sci 105:2108–2118. https://doi.org/10.3168/jds.2021-21121
10. Öztürk Doğan H, Albayrak ÖF (2023) Ag nanoparticles-decorated CuBi2O4-rGO electrodes as an amperometric sensor for electrochemical determination of Nitrite. Synth Met 298:117445. https://doi.org/10.1016/j.synthmet.2023.117445
11. Rashed MA, Ahmed J, Faisal M et al (2022) Surface modification of CuO nanoparticles with conducting polythiophene as a non-enzymatic amperometric sensor for sensitive and selective determination of hydrogen peroxide. Surf Interfaces 31:101998. https://doi.org/10.1016/j.surfin.2022.101998
12. Meng X, Xu Y, Zhang N et al (2021) Ferric hydroxide nanocage triggered Fenton-like reaction to improve amperometric immunosensor. Sens Actuators B Chem 338:129840. https://doi.org/10.1016/j.snb.2021.129840
13. Erdem A, Senturk H, Yildiz E, Maral M (2022) Amperometric immunosensor developed for sensitive detection of SARS-CoV-2 spike S1 protein in combined with portable device. Talanta 244:123422. https://doi.org/10.1016/j.talanta.2022.123422
14. Ortega-Valencia JE, Oliva-Ramírez J, García-Barradas O et al (2022) Development of a QCM immunosensor with functionalized gold nanoparticles for the detection of *Salmonella* Typhimurium. Mater Lett 314:131885. https://doi.org/10.1016/j.matlet.2022.131885
15. Teengam P, Siangproh W, Tontisirin S et al (2021) NFC-enabling smartphone-based portable amperometric immunosensor for hepatitis B virus detection. Sens Actuators B Chem 326:128825. https://doi.org/10.1016/j.snb.2020.128825
16. Su Z, Cheng Y, Xu X et al (2020) Preparation of porous thiolated polymer nanocomposite for construction of sensitive and selective phytohormone amperometric immunosensor. Microchem J 153:104380. https://doi.org/10.1016/j.microc.2019.104380
17. Wang Y, He X, Wang S et al (2024) Rapid detection of *Salmonella* Typhimurium in food samples using electrochemical sensor. LWT 206:116567. https://doi.org/10.1016/j.lwt.2024.116567
18. Castle LM, Schuh DA, Reynolds EE, Furst AL (2021) Electrochemical Sensors to detect bacterial foodborne pathogens. ACS Sens 6:1717–1730. https://doi.org/10.1021/acssensors.1c00481
19. Ávila Oliveira BD, Gomes RS, de Carvalho AM et al (2024) Revolutionizing food safety with electrochemical biosensors for rapid and portable pathogen detection. Brazilian J Microbiol 55:2511–2525. https://doi.org/10.1007/s42770-024-01427-6
20. de Brito FAE, Bezerra LCR, Furtado RF et al (2020) Pre-Collaborative Validation of an Amperometric Immunosensor for *Salmonella*. MDPI AG, p 43
21. Melo AMA, Furtado RF, de Fatima Borges M et al (2021) Performance of an amperometric immunosensor assembled on carboxymethylated cashew gum for *Salmonella* detection. Microchem J 167. https://doi.org/10.1016/j.microc.2021.106268
22. Kokkinos C, Economou A, Prodromidis MI (2016) Electrochemical immunosensors: critical survey of different architectures and transduction strategies. TRAC Trends Anal Chem 79:88–105. https://doi.org/10.1016/j.trac.2015.11.020
23. Pashazadeh P, Mokhtarzadeh A, Hasanzadeh M et al (2017) Nano-materials for use in sensing of *Salmonella* infections: recent advances. Biosens Bioelectron 87:1050–1064. https://doi.org/10.1016/j.bios.2016.08.012
24. Qasim almajidi Y, Althomali RH, Gandla K et al (2023) Multifunctional immunosensors based on mesoporous silica nanomaterials as efficient sensing platforms in biomedical and food safety analysis: a review of current status and emerging applications. Microchem J 191:108901. https://doi.org/10.1016/j.microc.2023.108901
25. Deb A, Nalkar GR, Chowdhury D (2023) Biogenic carbon dot-based fluorescence-mediated immunosensor for the detection of disease biomarker. Anal Chim Acta 1242:340808. https://doi.org/10.1016/j.aca.2023.340808
26. Lin Z, Cheng W, Liu C et al (2023) Coordination-induced self-assembly based carbon dot dendrimers as efficient signal labels

for electrochemiluminescent immunosensor construction. Talanta 254:124101. https://doi.org/10.1016/j.talanta.2022.124101
27. Ji C, Zhou Y, Leblanc RM, Peng Z (2020) Recent developments of Carbon dots in Biosensing: a review. ACS Sens 5:2724–2741. https://doi.org/10.1021/acssensors.0c01556
28. Wang J, Qiu J (2016) A review of carbon dots in biological applications. J Mater Sci 51:4728–4738. https://doi.org/10.1007/s10853-016-9797-7
29. de Oliveira BP, Bessa NU, de Nascimento C JF, et al (2023) Synthesis of luminescent chitosan-based carbon dots for *Candida albicans* bioimaging. Int J Biol Macromol 227:805–814. https://doi.org/10.1016/j.ijbiomac.2022.12.202
30. Liu Y, Huang H, Cao W et al (2020) Advances in carbon dots: from the perspective of traditional quantum dots. Mater Chem Front 4:1586–1613. https://doi.org/10.1039/D0QM00090F
31. Magar HS, Abdelghany H, Abbas MN et al (2023) Fast analysis of *Staphylococcus aureus* in food products using disposable label-free nano-electrochemical immunosensor chips. Microchem J 193:109097. https://doi.org/10.1016/j.microc.2023.109097
32. Melo AMA, Furtado RF, de Fatima Borges M et al (2021) Performance of an amperometric immunosensor assembled on carboxymethylated cashew gum for *Salmonella* detection. Microchem J 167:106268. https://doi.org/10.1016/j.microc.2021.106268
33. International Union of Pure and Applied Chemistry (2019) Limit of detection. The IUPAC Compendium of Chemical Terminology, 3rd edn. International Union of Pure and Applied Chemistry (IUPAC), Research Triangle Park, NC
34. Kansay V, Sharma VD, Chandan G et al (2023) Sustainable synthesis of nitrogen-doped fluorescent carbon quantum dots derived from *Cissus quadrangularis* for biomarker applications. Mater Chem Phys 296:127237. https://doi.org/10.1016/j.matchemphys.2022.127237
35. Passos Zattar AP, Paulo de Mesquita J, Pereira FV (2022) Luminescent carbon dots obtained from cellulose and their applications as sensors for metal ions. Mater Chem Phys 290:126633. https://doi.org/10.1016/j.matchemphys.2022.126633
36. Bhatt S, Bhatt M, Kumar A et al (2018) Green route for synthesis of multifunctional fluorescent carbon dots from Tulsi leaves and its application as cr(VI) sensors, bio-imaging and patterning agents. Colloids Surf B Biointerfaces 167:126–133. https://doi.org/10.1016/j.colsurfb.2018.04.008
37. Wang H, Su W, Tan M (2020) Endogenous fluorescence Carbon dots Derived from Food items. Innov 1:100009. https://doi.org/10.1016/j.xinn.2020.04.009
38. Long C, Jiang Z, Shangguan J et al (2021) Applications of carbon dots in environmental pollution control: a review. Chem Eng J 406:126848. https://doi.org/10.1016/j.cej.2020.126848
39. Zu F, Yan F, Bai Z et al (2017) The quenching of the fluorescence of carbon dots: a review on mechanisms and applications. Microchim Acta 184:1899–1914. https://doi.org/10.1007/s00604-017-2318-9
40. Manioudakis J, Victoria F, Thompson CA et al (2019) Effects of nitrogen-doping on the photophysical properties of carbon dots. J Mater Chem C Mater 7:853–862. https://doi.org/10.1039/C8TC04821E
41. Lu W, Gong X, Nan M et al (2015) Comparative study for N and S doped carbon dots: synthesis, characterization and applications for Fe3+probe and cellular imaging. Anal Chim Acta 898:116–127. https://doi.org/10.1016/j.aca.2015.09.050
42. Fan YZ, Zhang Y, Li N et al (2017) A facile synthesis of water-soluble carbon dots as a label-free fluorescent probe for rapid, selective and sensitive detection of picric acid. Sens Actuators B Chem 240:949–955. https://doi.org/10.1016/j.snb.2016.09.063
43. Ozyurt D, Kobaisi M, Al, Hocking RK, Fox B (2023) Properties, synthesis, and applications of carbon dots: a review. Carbon Trends 12:100276. https://doi.org/10.1016/j.cartre.2023.100276
44. Balanta MAG, da Silva Filho WJF, Souza MCG et al (2023) Deconvolution of photoluminescence spectra and electronic transition in carbon dots nanoparticles from microcrystalline cellulose. J Lumin 255:119607. https://doi.org/10.1016/j.jlumin.2022.119607
45. Nguyen V, Si J, Yan L, Hou X (2015) Electron–hole recombination dynamics in carbon nanodots. Carbon N Y 95:659–663. https://doi.org/10.1016/j.carbon.2015.08.066
46. Lin J, Huang X, Kou E et al (2023) Carbon dot based sensing platform for real-time imaging Cu2+distribution in plants and environment. Biosens Bioelectron 219:114848. https://doi.org/10.1016/j.bios.2022.114848
47. Raz J (2017) Carbon dots: Synthesis, Properties and Applications, 1st edn. Springer
48. Lv O, Tao Y, Qin Y et al (2016) Highly fluorescent and morphology-controllable graphene quantum dots-chitosan hybrid xerogels for in vivo imaging and pH-sensitive drug carrier. Mater Sci Engineering: C 67:478–485. https://doi.org/10.1016/j.msec.2016.05.031
49. Pandey FP, Rastogi A, Singh S (2020) Optical properties and zeta potential of carbon quantum dots (CQDs) dispersed nematic liquid crystal 4′- heptyl-4-biphenylcarbonitrile (7CB). Opt Mater (Amst) 105:109849. https://doi.org/10.1016/j.optmat.2020.109849
50. AMC technical briefAMC (1994) Is my calibration linear? Analyst 119:2363. https://doi.org/10.1039/an9941902363
51. Wang L, Xu A, Wang M et al (2023) Syringe-driven biosensing of *Salmonella* Typhimurium using nuclear track membrane filtration and nanozyme signal amplification. Food Control 152:109882. https://doi.org/10.1016/j.foodcont.2023.109882
52. Chen Q, Gao R, Jia L (2021) Enhancement of the peroxidase-like activity of aptamers modified gold nanoclusters by bacteria for colorimetric detection of. Talanta 221:121476. https://doi.org/10.1016/j.talanta.2020.121476
53. Vasan A, Geier R, Ingham SC, Ingham BH (2014) Thermal tolerance of O157 and non-O157 shiga toxigenic strains of *Escherichia coli*, *Salmonella*, and potential Pathogen surrogates, in Frankfurter Batter and Ground Beef of varying Fat levels. J Food Prot 77:1501–1511. https://doi.org/10.4315/0362-028X.JFP-14-106
54. Redemann MA, Brar J, Niebuhr SE et al (2018) Evaluation of thermal process lethality for non-pathogenic *Escherichia coli* as a surrogate for *Salmonella* in ground beef. LWT 90:290–296. https://doi.org/10.1016/j.lwt.2017.12.037
55. Zhang Y, Li Y, Wu W et al (2014) Chitosan coated on the layers' glucose oxidase immobilized on cysteamine/Au electrode for use as glucose biosensor. Biosens Bioelectron 60:271–276. https://doi.org/10.1016/j.bios.2014.04.035
56. Huang Y, Hara A, Terashima C et al (2019) Protein adsorption behavior on reduced graphene oxide and boron-doped diamond investigated by electrochemical impedance spectroscopy. Carbon N Y 152:354–362. https://doi.org/10.1016/j.carbon.2019.06.023
57. Latha BD, Soumya K, More N et al (2023) Fluorescent carbon quantum dots for effective tumor diagnosis: a comprehensive review. Biomedical Eng Adv 5:100072. https://doi.org/10.1016/j.bea.2023.100072
58. Tanwar A, Mukherjee A, Nath D et al (2023) Electrochemical Impedance Spectroscopy for studying fluorescence loss in immobilized Green fluorescent protein. J Photochem Photobiol Chem 445:115083. https://doi.org/10.1016/j.jphotochem.2023.115083
59. Canbaz MÇ, Sezgintürk MK (2014) Fabrication of a highly sensitive disposable immunosensor based on indium tin oxide substrates for cancer biomarker detection. Anal Biochem 446:9–18. https://doi.org/10.1016/j.ab.2013.10.014
60. Duan M, Li B, He Y et al (2024) A CG@MXene nanocomposite-driven E-CRISPR biosensor for the rapid and sensitive detection

of *Salmonella* Typhimurium in food. Talanta 266:125011. https://doi.org/10.1016/j.talanta.2023.125011
61. Wang Y, Ye Z, Ying Y (2012) New trends in Impedimetric biosensors for the detection of Foodborne pathogenic Bacteria. Sensors 12:3449–3471. https://doi.org/10.3390/s120303449

Publisher's note Springer Nature remains neutral with regard to jurisdictional claims in published maps and institutional affiliations.

Springer Nature or its licensor (e.g. a society or other partner) holds exclusive rights to this article under a publishing agreement with the author(s) or other rightsholder(s); author self-archiving of the accepted manuscript version of this article is solely governed by the terms of such publishing agreement and applicable law.

Authors and Affiliations

Rachel Menezes Castelo[1] · Marília de Albuquerque Oliveira[2] · Roselayne Ferro Furtado[3] · Bruno Peixoto de Oliveira[4] · Lucas Vinicius Leite Martoni[5] · Terezinha Feitosa Machado[6] · Celli Rodrigues Muniz[7] · Flávia Oliveira Monteiro da Silva Abreu[8] · Sérgio Antônio Spinola Machado[5] · Airis Maria Araújo Melo[9] · Huai N. Cheng[10] · Atanu Biswas[11] · Carlucio Roberto Alves[1]

✉ Roselayne Ferro Furtado
roselayne.furtado@embrapa.br

Rachel Menezes Castelo
rachel.menezes@aluno.uece.br

Marília de Albuquerque Oliveira
mariliaaoliveira7@gmail.com

Bruno Peixoto de Oliveira
bruno.peixoto@ufca.edu.br

Lucas Vinicius Leite Martoni
lucas.martoni@usp.br

Terezinha Feitosa Machado
terezinha.machado@embrapa.br

Celli Rodrigues Muniz
celli.muniz@embrapa.br

Flávia Oliveira Monteiro da Silva Abreu
flavia.monteiro@uece.br

Sérgio Antônio Spinola Machado
sasmach@iqsc.usp.br

Airis Maria Araújo Melo
airis.melo@ifpi.edu.br

Huai N. Cheng
hncheng100@gmail.com

Atanu Biswas
atanu.biswas@usda.gov

Carlucio Roberto Alves
carlucio.alves@uece.br

1 Centro de Ciências, Universidade Estadual do Ceará, CCT, Fortaleza, Brazil

2 Universidade Estadual do Ceará, Rede Nordeste de Biotecnologia– RENORBIO, Fortaleza, Brazil

3 Embrapa Agroindústria Tropical, Laboratório de Embalagens, Fortaleza, Brazil

4 Universidade Federal do Cariri, Instituto de Formação de Educadôres, Cidade Universitária, Brazil

5 Universidade de São Paulo, Instituto de Química de São Carlos, São Carlos, Brazil

6 Laboratório de Microbiologia, Embrapa Agroindústria Tropical, Fortaleza, Brazil

7 Laboratório de Microscopia Eletrônica, Embrapa Agroindústria Tropical, Fortaleza, Brazil

8 Laboratório de Polímeros Naturais, Universidade Estadual do Ceará, Fortaleza, Brazil

9 Departamento de Ensino, Instituto Federal do Piauí campus Picos, Picos, Brazil

10 Southern Regional Research Center, USD Agricultural Research Service, New Orleans, LA 70124, USA

11 USDA Agricultural Research Service, National Center for Agricultural Utilization Research, Peoria, IL 61604, USA